Mechanisms of self-diffusion in stoichiometric and substoichiometric amorphous silicon dioxide

Sergio Orlandini*
Consorzio Interuniversitario per le Applicazioni di Supercalcolo Per Università e Ricerca (CASPUR), Via dei Tizii 6, 00185 Roma, Italy and Università degli Studi di Roma "Sapienza," Piazzale Aldo Moro 5, 00185 Roma, Italy

Simone Meloni†
School of Physics, Room 126 UCD-EMSC, University College Dublin, Belfield, Dublin 4, Ireland

Mariella Ippolito‡
Consorzio Interuniversitario per le Applicazioni di Supercalcolo Per Università e Ricerca (CASPUR), Via dei Tizii 6, 00185 Roma, Italy

Luciano Colombo§
Dipartimento di Fisica, Università di Cagliari, I-09042 Monserrato (Ca), Italy and Sardinian Laboratory for Computational Materials Science (SLACS, CNR-INFM), Cittadella Universitaria, I-09042 Monserrato (Ca), Italy

(Received 20 May 2009; revised manuscript received 12 December 2009; published 11 January 2010)

We have investigated the Si and O self-diffusion in stoichiometric and substoichiometric amorphous SiO_2 by means of molecular-dynamics simulations. The diffusivity and the migration energies at different Si concentrations are reported and the results in qualitative agreement with previous experimental and theoretical (*ab initio*) results. We prove that the diffusion of Si and O occurs through steplike events. In particular, we identify three mechanisms, associated with coordination and "local stoichiometry" defects, responsible for the diffusion. The migration energy and pre-exponential factor, as well as the relative relevance of these mechanisms, is computed as a function of the Si concentration and temperature. A model for interpreting our results is proposed and discussed.

DOI: 10.1103/PhysRevB.81.014203 PACS number(s): 66.30.hh, 61.43.Bn

I. INTRODUCTION

Due to the shrinking of the size of transistors, the traditional methods of transferring data within and across devices has become the bottleneck for any further improvement of performance in microelectronics. Photonics, possibly based on silicon, has been identified as a viable solution for the problem. Unfortunately, due to its indirect gap, bulk silicon is a poor light emitter. However, it has been found that its optical properties improve when the dimension of the silicon structures become comparable with the wavelength of electrons.[1]

The experimental evidence of efficient light emission by silicon nanoparticles has paved the way for a technological leap. Silicon nanocrystals embedded in amorphous SiO_2 has emerged as the most promising material for this purpose.[2] Typically, this system is obtained by means of thermal cycles on a sample of Si-rich SiO_2 (hereafter indicated as SiO_{2-x}). Experiments[3] have shown that the emission efficiency of Si nanocrystal/amorphous SiO_2 (Si-nc/a-SiO_2) systems depends on the preparation of the sample, as this affects the structure of the system. Therefore, the understanding of the formation mechanism of Si-nc in a-SiO_2 is a key step in developing strategies for improving its optical properties.

Several authors suggest that the formation of nanoparticles is governed by the Ostwald ripening mechanism[4] and, in particular, by the diffusivity of Si atoms from smaller to larger nanoparticles. It was also found a strong dependency of the crystal growth from Si supersaturation, which seems to be in conflict with the Ostwald mechanism (Ref. 5, and reference therein). However, also in this case, this was considered an indication that the Si diffusion is the limiting step of the overall process. It would be therefore of particular interest to study the diffusivity of Si and its mechanism in stoichiometric and nonstoichiometric conditions. Unfortunately, to the best of our knowledge, no experimental studies on diffusion of Si in amorphous SiO_2 in absence of a Si/SiO_2 extended interfaces (i.e., in real conditions for the formation of nanoparticles) are available, especially concerning the identification of the mechanism of the diffusion. This is likely due to the fact that it is hard to generate a controlled concentration profile of isotopic Si into a bulklike sample (with no interface) so as to measure its variation upon thermal annealing. However, in a recent paper, Yu *et al.*[5] have addressed the identification of the atomistic mechanisms of diffusion of one excess Si atom in a-SiO_2 by performing *ab initio* calculations.

In this paper, the authors identified possible equilibrium sites and calculated the corresponding energy barrier for the diffusion of the excess Si atom by means of the nudged elastic band (NEB) method.[6] However, this investigation did not take into account neither the different concentrations of excess Si atoms nor the possible fluctuation of Si density within the samples. Finally, because of the use of NEB, the effect of temperature is not taken into account.

The aim of this paper is to study the diffusion mechanisms of Si and O in a-SiO_2 at different temperatures and for different Si-atoms' concentrations by means of classical molecular-dynamics (MD) simulations. We do not assume any *a priori* hypothesis on the mechanisms. Rather, by analyzing the MD trajectories we identify the set of most relevant mechanisms occurring at various thermodynamical and

 ©2010 The American Physical Society

chemical conditions. Finally, we calculate the contribution of each individual mechanism to diffusion and analyze the role of thermodynamical and chemical conditions.

The paper is organized as follows: in Sec. II we shortly revise the theoretical background of the calculation of diffusivity within MD and present a method for calculating the contribution of different mechanisms to the diffusivity. In Sec. III we describe the atomistic and the interaction model used in this paper. In Sec. IV A we present the results on the diffusivity and compare them with experimental and computational results available in literature. In Sec. IV B we analyze the contribution of a set of possible mechanism to the diffusivity of silicon. Finally, in Sec. V we draw the conclusions of this research.

II. THEORETICAL BACKGROUND

Solid-state self-diffusion is commonly due to several possible concurrent mechanisms, typically related to the presence and the dynamics of defects of different kind. For example, in crystals these defects typically are vacancy, self-interstitial, etc. Even though in amorphous materials the origin of self-diffusivity is less well understood, also in this case it is thought that it is induced by several concurrent mechanisms. Typically, however, the experimental interpretation of diffusivity-vs-temperature measurements is based on the phenomenological Arrhenius law,

$$D(T) = D_\infty \exp\left(-\frac{E}{k_b T}\right), \tag{1}$$

where D_∞ is the diffusivity at high temperature and E is the (average) migration energy, representing the (average) energy barrier to be overcome during diffusion. In Eq. (1) T and k_b represent the temperature and the Boltzmann constant, respectively. The theoretical atomic-scale investigation on self-diffusion is rather based on the calculation of the mean-square displacement (MSD), according to the Einstein random-walk equation

$$D(T) = \lim_{t\to\infty} \frac{1}{6} \frac{d\langle \Delta r^2(t)\rangle}{dt}, \tag{2}$$

where the $t \to \infty$ limit stands for simulations performed for long enough times. Equation (2) is straightforwardly implemented in MD since the MSD is defined as

$$\langle \Delta r^2(t)\rangle = \left\langle \sum_{i=1}^{N} [\vec{r}_i(t) - \vec{r}_i(0)] \right\rangle, \tag{3}$$

where $\vec{r}_i(t)$ and $\vec{r}_i(0)$ are the positions of the ith atom at time t and time 0, respectively, and it is therefore directly computed from the computer-generated atomic trajectories.

In addition, by means of Eq. (2) it is relatively easy to calculate the contribution to self-diffusion by each given mechanisms, provided that they are clearly identified. Once again, this information can be extracted by animation and inspection of atomic trajectories.

However, determining the contribution of each individual mechanism to the diffusivity is not trivial. In the following

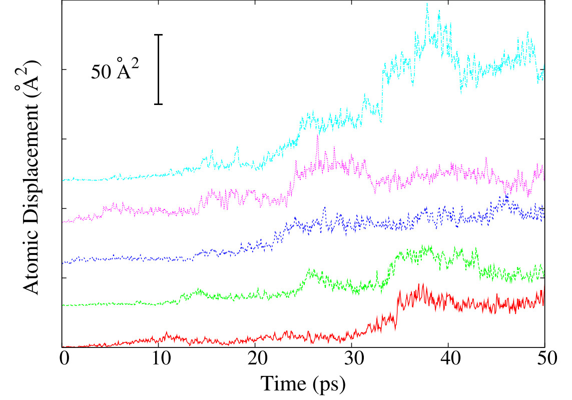

FIG. 1. (Color online) MSD displacement of few Si atoms selected randomly in the sample. The figure clearly shows that the diffusion occurs via stepwise events.

we shall demonstrate that under proper conditions the MSD is additive and therefore $D(T)$ is additive as well. We can therefore resort to Eq. (2) for calculating the $D(T)$ of each mechanism.

We assume that the diffusion occurs through a sequence of stepwise events. This assumption is justified by the empirical observation that indeed Si and O atoms diffuse through a stepwise mechanism in this material (see Fig. 1). We can therefore rewrite Eq. (3) as follows:

$$\langle \Delta r^2(t)\rangle = \left\langle \frac{1}{N}\sum_{i=1}^{N} \left[\sum_{\alpha=1}^{L} \Delta\vec{r}_i(t_\alpha) \right]^2 \right\rangle, \tag{4}$$

where L is the number of diffusive steps and $\Delta\vec{r}_i(t_\alpha)$ is the (vector) displacement of ith atom occurring at the time t_α. If the diffusive steps belong to different mechanisms, then Eq. (4) can be rewritten as follows:

$$\langle \Delta r^2(t)\rangle = \left\langle \frac{1}{N}\sum_{i=1}^{N} \left[\sum_{\alpha\in M_1} \Delta\vec{r}_i(t_\alpha) + \sum_{\beta\in M_2} \Delta\vec{r}_i(t_\beta) + \cdots \right]^2 \right\rangle, \tag{5}$$

where $\Delta\vec{r}_i(t_\alpha)$ is the displacement of ith atom due to an event of type M_1. An analogous definition is valid for $\Delta\vec{r}_i(t_\beta)$. The indexes α and β run over the set of events belonging to mechanism M_1 and M_2, respectively.

Equation (5) can be further manipulated as

$$\langle \Delta r^2(t)\rangle = \langle \Delta\vec{r}^2_{M_1}(t)\rangle + \langle \Delta\vec{r}^2_{M_2}(t)\rangle + \cdots + 2\langle \Delta\vec{r}_{M_1}(t)\cdot\Delta\vec{r}_{M_2}(t)\rangle + \cdots, \tag{6}$$

where

$$\langle \Delta r^2_{M_1}(t)\rangle = \left\langle \frac{1}{N}\sum_{i=1}^{N} \left[\sum_{\alpha\in M_1} \Delta\vec{r}_i(t_\alpha) \right]^2 \right\rangle \tag{7}$$

and

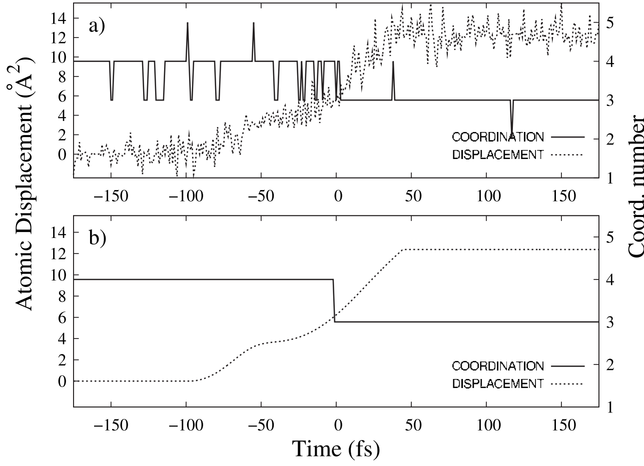

FIG. 2. Panel (a) $\Delta r_i^2(t)$ for a Si atom (dotted line) and the corresponding variation in the coordination number (continuous line). Panel (b) same data after time average over a time window τ. Values are reported with respect to average values in the period plotted.

$$\langle \Delta\vec{r}_{M_1}(t)\cdot\Delta\vec{r}_{M_2}(t)\rangle = \left\langle \frac{1}{N}\sum_{i=1}^{N}\sum_{\alpha\in M_1}\sum_{\beta\in M_2}\Delta\vec{r}_i(t_\alpha)\cdot\Delta\vec{r}_i(t_\beta)\right\rangle. \tag{8}$$

Similar definitions are assumed for other mechanisms.

If the sample is monophasic and there are no external fields acting on it, the product $\Delta\vec{r}_{M_1}(t_\alpha)\cdot\Delta\vec{r}_{M_2}(t_\beta)$ can assume with the same probability positive and negative values. Therefore, the term $\langle\Delta\vec{r}_{M_1}(t)\cdot\Delta\vec{r}_{M_2}(t)\rangle$ becomes zero. We verified that indeed this occurs in our simulations. In fact, the term $\langle\Delta\vec{r}_{M_1}(t)\cdot\Delta\vec{r}_{M_2}(t)\rangle$ is about three order of magnitude smaller than the smallest $\langle\Delta r^2_{M_\alpha}(t)\rangle$ term. Therefore, Eq. (6) reduces to

$$\langle\Delta r^2(t)\rangle \cong \langle\Delta r^2_{M_1}(t)\rangle + \langle\Delta r^2_{M_2}(t)\rangle + \cdots. \tag{9}$$

Equation (9) states that, under the above hypothesis, the total MSD is the sum of MSDs relative to each mechanism. Under the same hypothesis, Eq. (7) can be further simplified into

$$\langle\Delta r^2_{M_1}(t)\rangle \cong \frac{1}{N}\left\langle \sum_{i=1}^{N}\sum_{\alpha\in M_1}\Delta r_i^2(t_\alpha)\right\rangle. \tag{10}$$

We verified that also in this case the cross term $\langle\Sigma_i\Sigma_{\alpha,\alpha'}\Delta\vec{r}_i(t_\alpha)\cdot\Delta\vec{r}_i(t_{\alpha'})\rangle$ is negligible with respect to $\langle\Sigma_i\Sigma_\alpha\Delta r_i^2(t_\alpha)\rangle$ (about three order of magnitude smaller).

Unfortunately, $\Delta r_i^2(t)$ is noisy (see top panel of Fig. 2). This is due to the interplay of two phenomena: diffusive steps and atomic vibrations about equilibrium positions. The problem of the noise can be reduced by averaging the atomic positions on a time window τ centered on the time t. The window τ needs to be larger than the period of a vibration but not too large otherwise distinct diffusive steps can be confused. In our simulation we used a τ of 100 fs. The $\Delta r_i^2(t)$ computed on average positions is much more regular [compare Figs. 2(a) and 2(b)] and shows a clear stepwise behavior. The $\Delta r_i^2(t_\alpha)$ to be used in Eq. (10) is computed by the difference of average atomic positions before and after the time t_α.

A key issue is still open, namely, how to identify the times $t_\alpha, t_\beta, \ldots$ at which the events of type $M_1, M_2, \ldots$ occur. For each mechanism, we were able to identify order parameters $\theta_l(\vec{r}_1(t),\ldots,\vec{r}_N(t))$ that monitor the occurrence of a diffusive step. For example, let us assume that one diffusive mechanism implies the change in coordination number of a Si atom. By monitoring changes in the coordination number of each silicon we evaluate the total displacement of the mechanism, as indicated in Eq. (10) (see Fig. 2).

The complete description of the collective coordinates used for monitoring the mechanisms identified in this paper is given in Sec. IV B. Anticipating the results, we remark that using this technique we were able to identify a set of three mechanisms accounting for more than the 90% of the diffusivity.

On the basis of the so-computed MSD, we can calculate the diffusivity of each self-diffusion mechanism and, from this, the corresponding migration energy E_{M_α} and the pre-exponential factor $D_\infty^{M_\alpha}$. Of course, as for the overall E and D_∞, these are phenomenological parameters.

A somewhat related approach for the calculation of parameters governing the mass transport in crystals has been devised and applied by Da Fano and Jacucci.[7] In this approach, the frequency of events of a given type are counted and analyzed according to the following Arrhenius-type formula:

$$\Gamma_{M_\alpha}(T) = D_\infty^{M_\alpha}\exp\left(-\frac{E_{M_\alpha}}{k_bT}\right) = \nu_{M_\alpha}\exp(S_{M_\alpha}/k_b)\exp\left(-\frac{E_{M_\alpha}}{k_bT}\right), \tag{11}$$

where $\Gamma_{M_\alpha}(T)$ is the number of events of a give type, ν_{M_α} is the corresponding attempt frequency, E_{M_α} is the migration energy, and S_{M_α} is the migration entropy. In this case, Eq. (11), and therefore the parameters contained into it, is no longer phenomenological. Rather, it is derived from transition state theory in harmonic approximation.

It is worth mentioning that while the Da Fano and Jacucci method is perfectly justified in the case of crystals, where all the events of the same kind give the same contribution to the mass transport, in the case of amorphous materials the validity of this method is more questionable. In fact, depending on the environment of the atoms undergoing to a diffusive event, the corresponding displacement can vary significantly. This means that in the case of amorphous materials we must understand a diffusive mechanism in a more loose sense. However, in the following we have performed both kind of analysis and, anticipating our results, they both bring to the same qualitative conclusions.

III. MODEL AND COMPUTATIONAL SETUP

a-SiO_2 at various stoichiometries (from 33% to 45% of Si) was modeled by samples of size ranging from 5184 to 24 000 atoms. The stoichiometric a-SiO_2 sample was obtained by quenching from the melt. We started from a well-equilibrated sample of fluid SiO_2 at 8500 K. The density of

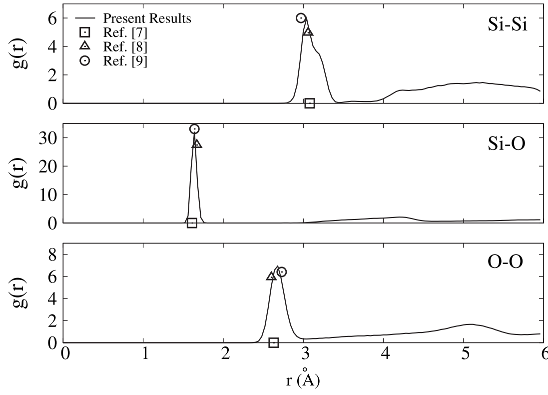

FIG. 3. Pair correlation function of stoichiometric a-SiO_2 as obtained from the quenching from the melt procedure described in the text. Positions and, when available, magnitudes of peaks as obtained in previous experimental [Johnson *et al.* (Ref. 8) and Susman *et al.* (Ref. 9)] and *ab initio* MD [Sarnthein *et al.* (Ref. 10)] works are reported for comparison.

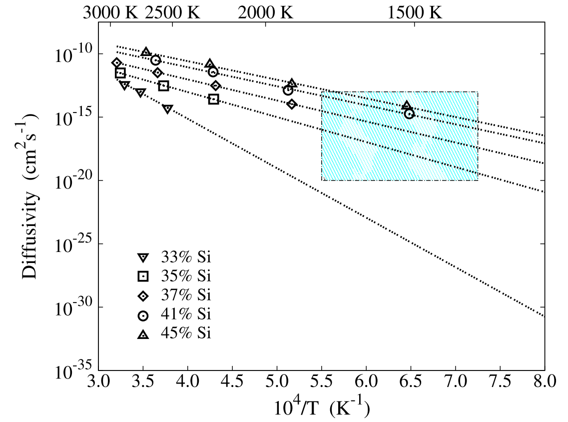

FIG. 4. (Color online) Diffusivity of Si atoms as a function of the inverse of temperature for SiO_{2-x} samples at various Si concentrations. The cyan frame in the graph represents the range of observed experimental values.

the sample was kept fixed at the experimental density of a-SiO_2 (2.17 g/cm^3). The sample was then cooled at a rate of 4×10^{13} K/s. and, finally, equilibrated for 80 ps at the target temperatures.

It is important to stress that, since the cooling rate is several order of magnitude higher than the experimental one, the consistency of our computational model with the experimental samples must be carefully checked. We compared the $g(r)$ (see Fig. 3) and $g(\theta)$ obtained with the above procedure with previous experimental[8,9] and *ab initio*[10] data, obtaining a very good quantitative agreement. In substoichiometric samples, O atoms were randomly replaced by Si atoms. After the substitution, the system was relaxed for 50 ps, with a time step of 0.5 fs, by mean of constant-temperature MD using the Nosè-Hoover chain method.[11] Since the experimental density is not available, we kept the density of these systems fixed at the density of a-SiO_2. However, we verified that with this setup the internal pressure of such samples is negligible.

We investigated the diffusion in a range of temperature from 1500 to about 3000 K, depending from the concentration of Si. Total and mechanism specific MSD of Eqs. (3)–(6) are computed by means of MD at constant number of particles, volume and energy. Simulations at different temperatures were performed changing the total energy of the system. At each concentration and temperature, we run 200 ps MD simulations. We verified that such long simulations are adequate for reaching the linear regime of the MSD required by Eq. (2).

The atomic interactions were treated by means of the modified Tersoff potential recently developed by Billeter *et al.*[12] Here we want simply to stress that this potential contains two- and three-body terms and that these interactions are affected by the environment of the interacting atoms through an effective coordination number of each of them. Electrostatic interactions are not included in this model and this makes it suitable for large-scale simulations. Previous works have shown that this potential is able to correctly reproduce several properties of SiO_2 and Si/SiO_2 systems.[12–14] In particular, we tested the ability of the Billeter *et al.* potential in reproducing the energetics and the path for the vacancy-mediated diffusion in crystalline SiO_2. We started from the NEB trajectory obtained by Laino *et al.*[15] based on an *ab initio* force model. We performed a NEB simulation using the Billeter *et al.* potential finding a migration energy which is the 80% of that found by Laino *et al.* The agreement between classical and *ab initio* configurations along the NEB trajectory is even better, being the maximum difference in the bond lengths lower than 3%.

IV. RESULTS AND DISCUSSION

A. Migration energy

Figure 4 shows the diffusivity of Si atoms at various temperatures and Si concentrations as obtained from MSD (see Sec. II). Corresponding data for O were computed as well but not shown in figure as there are no corresponding experimental data to compare with. It is worth noticing that we performed MD simulations in a temperature range higher than the experimental one. This is a standard method for accelerating MD simulations for studying diffusivity. In particular, under the only hypothesis of an Arrhenius dependence upon temperature (a very widely and common-sense assumption, indeed) high-temperature data can safely be extrapolated down to room temperature. Of course the reliability of the results must be checked *a posteriori*. In the present case, we have performed two tests: (i) assessing whether the system was still in amorphous phase at the higher temperatures; (ii) assessing whether the diffusion data extracted from such a sample can be extrapolated at lower temperatures. As for (i), by analyzing the $g(r)$ we verified that the system persisted in the amorphous phase also at the higher temperatures. This is not surprising as in simulations, especially constant volume simulations of (relatively) small samples, large fluctuations of the density are forbidden and the system can stay in a metastable state despite the fact that exist another phase at lower free energy. As for (ii), we verified that the log of diffusivity is inversely proportional to the temperature

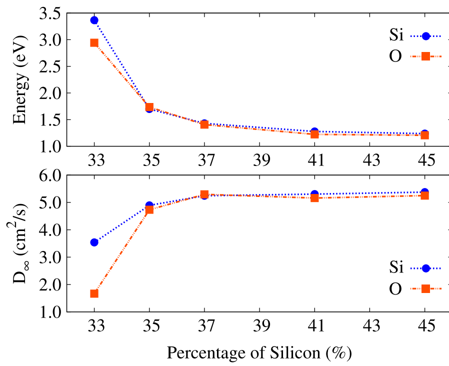

FIG. 5. (Color online) Si and O migration energy (top panel) and pre-exponential factor D_∞ (bottom panel) as a function of the Si concentration.

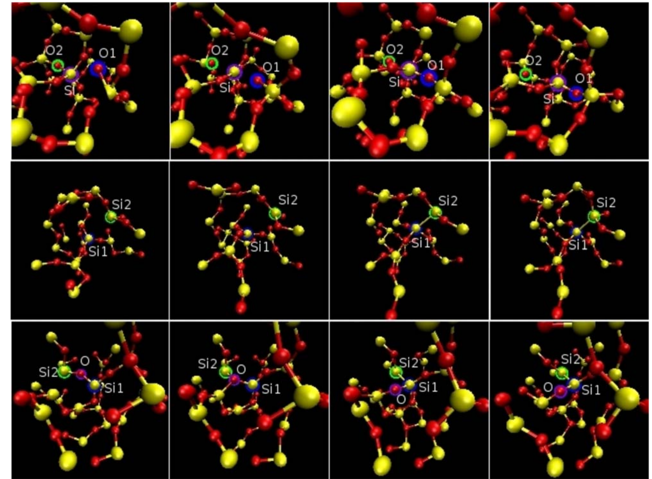

FIG. 6. (Color online) Snapshots of events belonging to the O-driven mechanism (top), Si-driven mechanism (center), and bond-swapping mechanism (bottom). The mechanisms are described in detail in the text. Atoms involved in the processes are highlighted in green, blue, and violet and identified by Si and O symbols (followed by numbers when more than one atom of the same chemical species is involved in the process).

over the whole range of temperature simulated, as requested from the Arrhenius law. For sake of comparison, we also report the $D(T)$ vs T range of experimental data[16–19] (the cyan box in Fig. 4). It can be seen that extrapolated computational data are well within the experimental range, confirming the overall agreement of the present results with experimental data.

From Fig. 4 and the corresponding data for the diffusion of O, we calculated migration energies as a function of the Si concentration [see Fig. 5, top]. For the migration energy of Si at the stoichiometric composition we found a value that is the 65–75 % of the experimental values,[16–19] depending on the considered experiments. These results are in line with the predictive capability of the Billeter *et al.* potential, as evaluated by the test of diffusion in α quartz (see Sec. III), and the typical accuracy of diffusivity calculated by means of classical MD.

We also remark that there exists a relevant difference between the present simulations and the experimental setup. The experimental diffusivity is calculated by fitting the concentration distribution of radioactive Si atoms in a sample of SiO_2. The radioactive Si is provided by a sample of crystalline Si through a Si/a-SiO_2 interface. The diffusivity is therefore due to a possible two-step mechanism: (i) crossing of the Si/a-SiO_2 interface and (ii) diffusion in a-SiO_2. Moreover, these experiments are performed in nonequilibrium conditions. So, the experimental conditions, which are meant to study the diffusivity occurring in different kind of systems, are not directly mimicked by our simulations.

Finally, our results are in qualitative agreement with previous density functional theory (DFT) calculations,[5] which report an energy barrier of 4.5–5 eV. However, also in this case it is worth noticing some difference in the setup. In fact, the DFT calculations were carried out by guessing a diffusion path composed of several steps. The atomistic model for simulating each of these steps was indeed a cluster model, therefore elastic forces due to the condensed phase environment were neglected. Moreover, even though the authors mention that the diffusion energy changes from one initial/final site to another of the same type, results are reported only for one of them. In addition, the small size of the sample (just 24 SiO_2 units) does not allow neither the fluctuation of the (local) density nor of the (local) chemical composition of the sample. Since migration energy is affected by the concentration (see below), results might change in function of these fluctuations. Furthermore, since just one path has been tested, results of Yu *et al.*[5] might be strongly biased by the only mechanism actually considered.

As for the stoichiometry of the sample, Fig. 4 shows an increase in diffusion of Si with its concentration. This is reflected by a decrease in the migration energy E (see Fig. 5, top) and by an increase in the pre-exponential coefficient D_∞ (see Fig. 5, bottom). This trend is in agreement with experimental findings.[16] It is interesting to note that a similar trend is observed for the diffusion of O as well. This seems to suggest that the diffusion of O and Si atoms is indeed correlated.

B. Mechanisms

In this paragraph we shall identify the diffusion mechanism of silicon and its dependence on the stoichiometry of the sample. By visual inspection of the trajectories we identified three types of stepwise mechanisms (see Sec. II) which can be described in terms of change in coordination for Si and O atoms or swapping of a Si-Si bond for a Si-O bond (or vice versa). Please notice that, at a variance from previous papers,[5] our model does not take into account the actual value of the coordination number, rather its variation. The rationale for this choice is that in amorphous samples there might exist many different configurations, all undergoing to one of the mechanisms introduced above.

More in detail, the first mechanism consists of the change in coordination of O atoms. An example of such an event is presented in the top panel of Fig. 6. In this diffusive event an O atom which is initially onefold coordinated (the blue atom labeled "O1" in the panel) recovers its complete coordination by forming a bond with a Si atom (the violet atom labeled

"Si" in the panel). In order to do so, the Si atom breaks a bond with another O (the green atom labeled "O2" in the same panel) which therefore becomes onefold coordinated. We refer hereafter to this mechanism as O driven. Of course, events with O and Si atoms with different initial and final coordination, all belonging to the O-driven mechanism, occur in our simulations. The second kind of mechanism is analogous to the first one but for that in this case Si atoms change their coordination. An example of such an event is shown in the central panel of Fig. 6. Here, two Si atoms are initially threefold coordinated (blue and green atoms labeled "Si1" and "Si2," respectively, in the panel). By forming a bond among them they change their coordination from 3 to 4 so restoring their perfect coordination. We refer hereafter to this mechanism as Si driven. As above, events with O and Si atoms with different initial and final coordination, all belonging to the Si-driven mechanism, occur in the simulation. Finally, in the third kind of mechanism a Si-Si bond is swapped for a Si-O bond (or vice versa). An example of this mechanism is presented in the bottom panel of Fig. 6. In this event, the green Si (labeled Si2 and the violet O (labeled "O") are initially bonded. After the swapping the green Si atom is bonded to the blue Si (labeled Si1). We shall refer to this mechanism as bond swapping. A possible explanation of the behavior described above is the attempt of miscoordinated Si and O atoms to restore the optimal coordination (O-driven and Si-driven mechanisms) or to establish a network of chemical bonds that minimize the stress in a region of the sample (bond swapping).

In order to implement the method described in Sec. II we need to identify collective variables able to monitor the occurrence of events of the above types. For this purpose we use total and partial coordination numbers. The former counts the total number of neighbors of a given atom while the latter takes into account also their chemical nature. Mathematically, the partial coordination number if defined as

$$\theta_i^B = \sum_{j \in B} \Theta(r_{ij} - r_{cut}), \tag{12}$$

where θ_i^B is the coordination number of the ith atom with respect to atoms of the species B, $\Theta(r - r_{cut})$ is the Heaviside step function, r_{ij} is the distance between atom i and atom j, and r_{cut} is the cutoff distance beyond which two atoms are no longer considered bonded. The sum in Eq. (12) runs over atoms of the chemical species B. The total coordination number can be obtained from partial coordination number according to the following formula:

$$\theta_i = \sum_{B=1}^{N_{sp}} \theta_i^B, \tag{13}$$

where the sum runs over the N_{sp} chemical species in the sample (two in the present case).

The O-driven mechanism can be monitored following the variation in the total coordination number of the O atoms (hereafter referenced by the symbol θ_O). It is worth mentioning that analyzing the partial coordination numbers we discovered that θ_O^O (number of O atoms bonded to O atoms) is always zero. This means that under the condition of the present simulations O_2 molecules are never formed. Similarly, we identify events belonging to the Si-driven mechanism monitoring changes in the value of total coordination of Si atoms (θ_{Si}). Finally, we use partial coordination θ_{Si}^O and θ_{Si}^{Si} for identifying events in which a Si-O bond is swapped for a Si-Si bond (or vice versa), under the constrain that the total coordination number of the atom considered is unchanged ($\Delta\theta_{Si}^O + \Delta\theta_{Si}^{Si} = 0$).

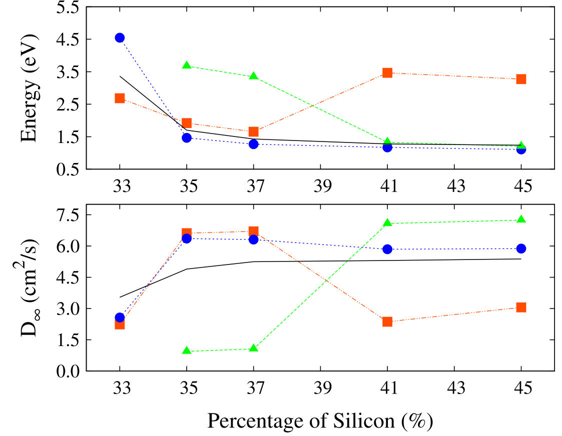

FIG. 7. (Color online) O-driven (red squares), Si-driven (blue dots), and bond-swapping (green triangles) migration energies E_{M_α} and pre-exponential factor $D_\infty^{M_\alpha}$ as computed by the diffusivity $D^{M_\alpha}(T)$ defined in Sec. II. The solid (black) lines without symbols represent the total migration energy and pre-exponential factor of Si (see Fig. 5).

Using these collective variables we can identify the time at which events of a given mechanism occur. The change in collective variables θ_i^B and θ_i also indicates that the atom i (and possibly the atoms bonded to it) is involved in the diffusive step. Then, applying Eq. (10) on these atoms, distinguishing between Si and O, we compute the MSD displacement relative to a given mechanism and the corresponding diffusivity. We remark that the three mechanisms introduced above account for more than the 90% of the total MSD at all temperatures and Si concentrations.

From the so-computed MSD we can calculate the $D_{M_\alpha}(T)$ of each individual mechanism and, from this, the corresponding E_{M_α} and $D_\infty^{M_\alpha}$. In Fig. 7 are reported E_{M_α} and $D_\infty^{M_\alpha}$ at various stoichiometries. For comparison, in Fig. 8 we report the corresponding data obtained through the Da Fano and Jacucci method.[7] Our calculations [Fig. 7, top] show that at lower Si concentration the mechanism with the lowest migration energy is the O-driven mechanism. When the Si concentration is increased, the activation energy of the Si-driven and bond-swapping mechanisms is reduced below that of the O-driven mechanism which, for a Si concentration above 37%, rises. Concerning the pre-exponential factor, for Si concentration below 39% the $D_\infty^{M_\alpha}$ of Si-driven and O-driven mechanisms is about the same [see Fig. 7, bottom]. However, above this value, the $D_\infty^{M_\alpha}$ of the O-driven mechanism is largely reduced.

An equivalent analysis performed on the basis of Eq. (11) taken from Da Fano and Jacucci[7] produced results in qualitative agreement with those obtained from the MSD of each

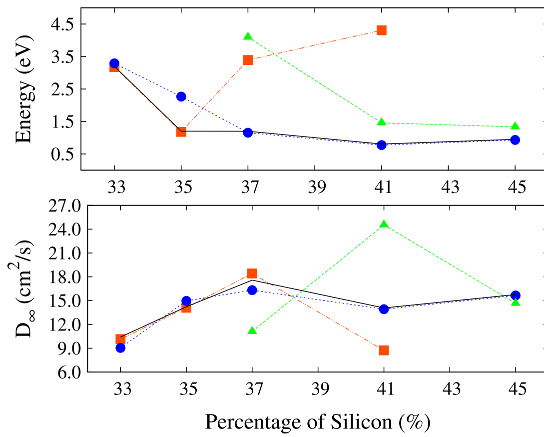

FIG. 8. (Color online) O-driven (red squares), Si-driven (blue dots), and bond-swapping (green triangles) migration energies E_{M_α} and pre-exponential factor $D_\infty^{M_\alpha}$ computed according to Ref. 7.

individual mechanism (see above). E_{M_α} and $D_\infty^{M_\alpha}$ obtained from Eq. (11) are reported in Fig. 8. It can be seen that, as in the case of Fig. 7, the migration energy of the O-driven mechanism rises for higher Si concentration. At the same time, the migration energy of the Si-driven and bond-swapping mechanisms both decrease.

It is also interesting to determine the relevance of each mechanism with respect to the total diffusivity at the given temperature and Si concentration. In Fig. 9 we report the relative occurrence of the $D(T)$ due to each of the three mechanisms [hereafter referred to as $\%D(T)$] as a function of the stoichiometry of the samples at few selected temperatures. A similar trend is observed in the whole range of temperature considered in this paper (1500–3000 K). For temperature below 1500 K, we calculated the $\%D(T)$ on the basis of data extrapolated from the E_{M_α} and $D_\infty^{M_\alpha}$ of each mechanism, both using our method and the method of Da Fano and Jacucci. These results are shown in Fig. 10.

Figure 9 shows that in stoichiometric conditions the O-driven mechanism is the dominating one. However, as the Si concentration increases, the Si-driven mechanism becomes the most relevant. At low temperatures ($T \leq 2300$ K), already an increase in Si concentration as low as 2% has a dramatic effect on the fraction of diffusivity due to Si and O undercoordination. At higher temperatures ($T \geq 2600$) this effect is less evident. For example, at 3000 K and a %Si=35%, the contribution of Si-driven and O-driven mechanisms is about the same. Concerning the bond-swapping mechanism, its contribution to the diffusivity is negligible for Si concentration <37–41%. At higher Si concentrations (≥41%) it becomes active, reaching a level of contribution to the diffusivity as high as 15–20 %.

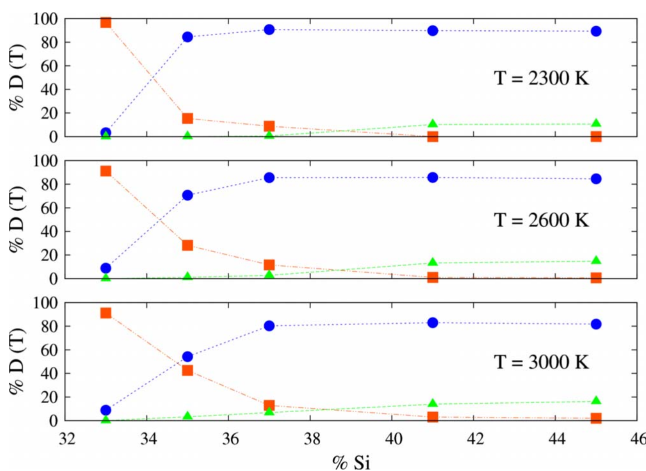

FIG. 9. (Color online) Relative contribution to the total diffusivity due to O-driven (red squares), Si-driven (blue dots), and bond-swapping (green triangles) mechanisms.

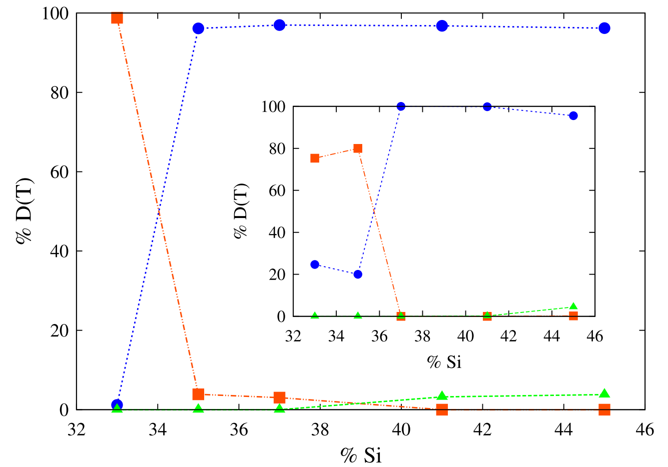

FIG. 10. (Color online) Relative contribution to the total diffusivity due to O-driven (red squares), Si-driven (blue dots), and bond-swapping (green triangles) mechanisms. In the inset we report the same quantities calculated according to Eq. (11) taken from Ref. 7.

Overall the above results substantiate a robust model for diffusion in stoichiometric and nonstoichiometric a-SiO_2. In systems close to stoichiometric SiO_2(%Si≤35%) there is a natural abundance of Si and O coordination defects. However, while threefold-coordinated Si atoms are rather stable onefold-coordinated O are not. Therefore, an higher number of defective O will undergoes to stepwise diffusive events aimed at restoring their perfect coordination and this causes the stepwise diffusive events observed in our simulations. Concerning the bond-swapping mechanism, it is not effective in causing the diffusivity as very few and stable Si-Si bonds are either present or can be formed at a low Si concentration.

At variance, for higher Si concentrations the overall amount of defects present in the samples, both of coordination or "local" stoichiometry nature, is higher and this increases the Si diffusivity. However, due to the overabundance of Si, the amount of defective O atoms is reduced. This fact reduces the contribution of the corresponding mechanism to the diffusivity. On the contrary, the amount of defective Si is increased and therefore the Si-driven mechanism is more effective at these concentrations. At the same time, the concentration of Si-Si bonds is also increased which induce an increase in the diffusivity due to the bond-swapping mechanism.

Finally, as for the thermodynamical conditions, the effect of the temperature is to level the contributions of the various mechanisms to the diffusivity. This is consistent with our

model as, at higher temperatures, energetically less favored defects become more abundant and therefore the corresponding mechanisms become more effective.

V. CONCLUSIONS

In this paper we have analyzed the diffusion mechanism in SiO_{2-x} samples at various Si concentrations and at different temperatures using classical molecular-dynamics simulations based on the Billeter *et al.*[12] model potential. We have demonstrated that this potential is able to produce results in reasonable agreement with previous experimental and theoretical works. In particular, we have found that the increase in Si concentration increases the diffusivity of Si, in agreement with experiments.

We have investigated the Si diffusion process and we have identified a set of mechanisms which might be responsible for this phenomenon in SiO_{2-x}. In particular, we have identified that the three most important mechanisms governing the diffusion are: (i) the tendency of undercoordinated O atoms to restore the complete coordination, (ii) the tendency of undercoordinated Si atoms to restore the complete coordination, and (iii) the swapping of Si-O bonds for Si-Si bonds (and vice versa). This behavior has been interpreted in terms of the abundance of defects compatible with the identified mechanisms. In order to measure the contribution of each of them to the diffusivity, we have developed a method to compute the diffusivity associated each mechanism. Using this technique, we were able to demonstrate that at low Si concentration the O-driven mechanism is responsible for the diffusion of Si while at higher concentration the diffusion is due to the Si-driven and bond-swapping mechanisms.

These results, and, in particular, the dependency of the relative relevance of the various mechanisms on the Si concentration and the thermodynamical conditions, suggest two main conclusions: (i) a single diffusion path is not adequate for describing this phenomenon as it might depend on the local Si concentration (fluctuations of stoichiometry might occur in real samples) and (ii) temperature deeply affects the diffusion mechanism.

ACKNOWLEDGMENT

One of us (L.C.) acknowledges financial support by "Fondazione Banco di Sardegna."

*s.orlandini@caspur.it

†Permanent address: Consorzio Interuniversitario per le Applicazioni di Supercalcolo Per Università e Ricerca (CASPUR), Via dei Tizii 6, 00185 Roma, Italy; simone.meloni@caspur.it

‡m.ippolito@caspur.it

§luciano.colombo@dsf.unica.it

[1] L. T. Canham, Appl. Phys. Lett. **57**, 1046 (1990).
[2] L. Pavesi, L. Dal Negro, C. Mazzoleni, G. Franzò, and F. Priolo, Nature (London) **408**, 440 (2000).
[3] F. Iacona, G. Franzò, and C. Spinella, J. Appl. Phys. **87**, 1295 (2000).
[4] Y. Q. Wang, R. Smirani, G. G. Ross, and F. Schiettekatte, Phys. Rev. B **71**, 161310(R) (2005).
[5] D. Yu, G. S. Hwang, T. A. Kirichenko, and S. K. Banerjee, Phys. Rev. B **72**, 205204 (2005).
[6] G. Henkelman, B. P. Uberuaga, and H. Jónsson, J. Chem. Phys. **113**, 9901 (2000).
[7] A. Da Fano and G. Jacucci, Phys. Rev. Lett. **39**, 950 (1977).
[8] P. A. V. Johnson, A. C. Wright, and R. N. Sinclair, J. Non-Cryst. Solids **58**, 109 (1983).
[9] S. Susman, K. J. Volin, D. L. Price, M. Grimsditch, J. P. Rino, R. K. Kalia, P. Vashishta, G. Gwanmesia, Y. Wang, and R. C. Liebermann, Phys. Rev. B **43**, 1194 (1991).
[10] J. Sarnthein, A. Pasquarello, and R. Car, Phys. Rev. B **52**, 12690 (1995).
[11] G. J. Martyna, M. L. Klein, and M. Tuckerman, J. Chem. Phys. **97**, 2635 (1992).
[12] S. R. Billeter, A. Curioni, D. Fischer, and W. Andreoni, Phys. Rev. B **73**, 155329 (2006).
[13] D. Fischer, A. Curioni, S. Billeter, and W. Andreoni, Appl. Phys. Lett. **88**, 012101 (2006).
[14] M. Ippolito, S. Meloni, and L. Colombo, Appl. Phys. Lett. **93**, 153109 (2008).
[15] T. Laino, D. Donadio, and I.-Feng W. Kuo, Phys. Rev. B **76**, 195210 (2007).
[16] D. Mathiot, J. P. Schunck, M. Perego, M. Fanciulli, P. Normand, C. Tsamis, and D. Tsoukalas, J. Appl. Phys. **94**, 2136 (2003).
[17] T. Takahashi, S. Fukatsu, K. M. Itoh, M. Uematsu, A. Fujiwara, H. Kageshima, Y. Takahashi, and K. Shiraishi, J. Appl. Phys. **93**, 3674 (2003).
[18] D. Tsoukalas, C. Tsamis, and P. Normand, J. Appl. Phys. **89**, 7809 (2001).
[19] M. Uematsu, H. Kageshima, Y. Takahashi, S. Fukatsu, K. M. Itoh, K. Shiraishi, and U. Gösele, Appl. Phys. Lett. **84**, 876 (2004).